ISBN: 978-3-95450-204-2 ISSN: 2673-5350 doi:10.18429/JACoW-IBIC2019-TUPP044

# MULTIPLE SYNCHROTRON LIGHT MONITORS FOR TRANSVERSE MATCHING AND MONITORING AT CEBAF

B.G. Freeman, J. Gubeli, and M.G. Tiefenback, Jefferson Lab, Newport News, VA, USA

*Abstract*

Beam setup at the Continuous Electron Beam Accelerator Facility (CEBAF) involves threading beam through the machine and monitoring global transfer functions to identify and address cumulative lattice errors. Transverse beam emittance may grow by as much as two orders of magnitude, mediated by synchrotron radiation. Re-matching the enlarged beam phase space into successive re-circulation arcs minimizes this emittance growth but requires knowledge of the actual beam distribution. This is now accomplished through quadrupole scans using wire profile monitors, the most time-consuming activity in our setup process. We propose to use Synchrotron Light Monitors (SLMs) to image the beam at homologous points in the four super-period re-circulation arc lattices. Benefits include real-time monitoring of beam parameters and reduced elapsed time for initial setup. These SLMs will be installed in Arc 7 of the CEBAF machine, where Synchrotron Radiation contributes moderately to emittance growth. One of four required SLMs will be installed and commissioned this year, with the rest being installed next year.

## INTRODUCTION

The vision in 1986 for CEBAF was to use Synchrotron Radiation to measure the beam emittance [1]. Certain challenges presented in this CEBAF technical note are easily solved now with newer technologies and improved performance. Challenges such as filtering, camera resolution, digitization of the image, and diffraction limitations were all discussed in the note. Now, thirty years and a major energy upgrade later, such devices will be implemented for CEBAF.

The CEBAF machine has several SLMs now, used for monitoring of the beam energy, energy stability, and RF cavity gradient and phase stability. Our principal SLMs are in the high-dispersion regions to monitor energy stability and obtain information about the longitudinal distribution of the beam [2].

The emittance growth for a given Arc depends on the transverse mismatch of the beam to the periodic lattice functions. The proposed four point SLM based measurement should provide an efficient and non-destructive means to measure and monitor the beam properties.

## MATCHING TECHNIQUES

### *Existing Measurement Methods*

The present method for measuring and matching the transverse beam properties of the electron beam uses wire profile monitors, or wire scanners. These devices provide great resolution of our small $\sigma < 100 \times 100$ μm beam sizes. The profile scans are relatively slow and can take minutes. We vary the strength of a quadrupole in the non-dispersive region upstream of each Arc, and measure the resulting beam size [3]. This process can be time consuming, depending strongly on the speed of wire insertion and details of data collection protocol. We have to balance the insertion velocity against the noise in the measurement. Determination of the range of focusing strength needed can be time consuming. We target measurements spanning the waist (minimum size) and up to a factor of three times greater for both stronger and weaker settings. Upstream optics in some cases must be modified to accommodate strength limitations for the quadrupole being varied. Problematic cases can require several hours to measure and rematch one of the ten Arcs.

Improvements have been made through the years to the process, as well as to software tools for data collection and analysis. The suite of tools, which is called `qsUtility` [4], makes use of Self Describing Data Files (SDDS) [5] to transport the data to `elegant` [6]. The enhancements have improved reproducibility of the measurements, and have improved the speed at which the data can be obtained and analyzed. We plan to use the existing tool suite to analyze the data and compare the measured Twiss parameters for agreement.

### *Four-point SLM-based Method*

The CEBAF accelerator consists of two anti-parallel superconducting RF linacs connected by ten 180° Arc bends to guide the beam successively through the linacs for energy gain. CEBAF is capable of providing up to 12 GeV electrons to experimental Hall D and 11 GeV electrons to halls A, B, and C.

CEBAF can be configured to provide beam to halls A, B or C after each pass through the linacs. Arc 7 contains the second-highest beam energy in the East Arcs. Arc 7 was chosen for this initial SLM installation, as most of the scheduled experimental plans require beam to pass though this Arc. In this Arc, Synchrotron Radiation contributes moderately to emittance growth. Each Arc consists of a periodic focusing structure of single or paired dipole magnets separated by alternating singlet and triplet groups of quadrupole magnets, Arc 7 consists of thirty-three quadrupoles and sixteen pairs of 3 $m$ long dipoles. The homologous points of the four super-periods are chosen to be as close as practical to the horizontal dispersion zeroes just downstream of the 8th, 16th, 24th and 32nd dipoles. The mechanical layout of this Arc allowed for one design to be implemented at all four locations. The horizontal and vertical dispersion and betatron plots for the chosen 7th Arc can be seen in Fig. 1 and Fig. 2

ISBN: 978-3-95450-204-2 ISSN: 2673-5350 doi:10.18429/JACoW-IBIC2019-TUPP044



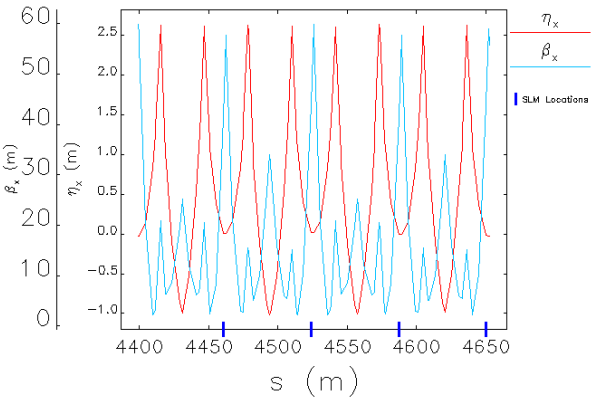


Figure 1: Horizontal Dispersion ($\eta_x$) and Beta ($\beta_x$) Functions. SLM locations marked with Dark Blue lines.

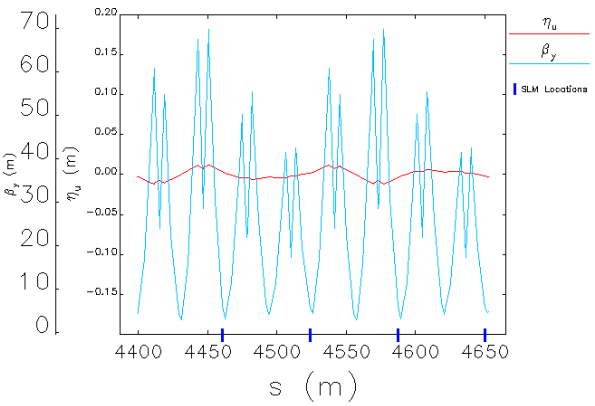


Figure 2: Vertical Dispersion ($\eta_y$) and Beta ($\beta_y$) Functions. SLM locations marked with Dark Blue lines.

### *Theory and Benefits*

Other facilities have done similar four point measurements using Optical Transition Radiation (OTR), such as implemented at the Accelerator Test Facility at KEK in Japan [7] and at the VUV-FEL at DESY in Hamburg, Germany [8]. In both cases the measured beam profiles from the OTR monitors were used to solve for the Twiss parameters using methods described in Chapter 4 of *Measurement and Control of Charged Particle Beams* [3], called Multiple Wire Measurement [3]. This method consists of solving the matrix equation

$$\begin{pmatrix} \left(\sigma_x^{(1)}\right)^2 \\ \left(\sigma_x^{(2)}\right)^2 \\ \left(\sigma_x^{(3)}\right)^2 \\ \vdots \\ \left(\sigma_x^{(n)}\right)^2 \end{pmatrix} = \begin{pmatrix} \left(R_{11}^{(1)}\right)^2 & 2R_{11}^{(1)}R_{12}^{(1)} & \left(R_{11}^{(1)}\right)^2 \\ \left(R_{11}^{(2)}\right)^2 & 2R_{11}^{(2)}R_{12}^{(2)} & \left(R_{11}^{(2)}\right)^2 \\ \left(R_{11}^{(3)}\right)^2 & 2R_{11}^{(3)}R_{12}^{(3)} & \left(R_{11}^{(3)}\right)^2 \\ \vdots & \vdots & \vdots \\ \left(R_{11}^{(n)}\right)^2 & 2R_{11}^{(n)}R_{12}^{(n)} & \left(R_{11}^{(n)}\right)^2 \end{pmatrix} \begin{pmatrix} \beta(s_0)\epsilon \\ -\alpha(s_0)\epsilon \\ \gamma(s_0)\epsilon \end{pmatrix} \quad (1)$$

for $\epsilon$, $\beta(s_0)$, and $\alpha(s_0)$ which can be fitted by a least-squares fit, as is already done with our current suite of tools [4]. In Eq. (1), the superscript index in parentheses refers to the measurement step, the super-index 2 is meant to denote the square of $R_{mn}^{(n)}$ transfer matrix elements from the design. The left hand $\left(\sigma_x^{(n)}\right)^2$ elements are the measured profiles from the four monitors. This works for single wire profile measurement and also for multiple profiles taken at different locations [3]. As written, the emittance is presumed constant across all measurements. We will initially approximate the emittance variation intrinsic to our application by the anticipated growth of the matched model. One could also solve for $\epsilon$, given

$$\Sigma_x = \left\{ \left(\sigma_x^{(1)}\right)^2, \left(\sigma_x^{(2)}\right)^2, \ \ldots \ , \left(\sigma_x^{(n)}\right)^2 \right\},$$

then $\epsilon = \sqrt{\det \Sigma_{beam}}$ [3]. The final step is to solve for $\alpha = -\Sigma_{12}/\epsilon$, $\beta = \Sigma_{11}/\epsilon$, and $\gamma = \Sigma_{22}/\epsilon$ [3]. Where $\epsilon$, $\beta$, and $\alpha$ are the normal definitions of the Twiss parameters. The $\alpha$ is related to the tilt of the beam, or the extent that the beam is converging or diverging. The $\beta$ is related to the size and shape of the beam. The $\epsilon$ is related to the beam size and describes the area of the phase ellipse $A = \pi \cdot \epsilon$.

Four on-line non-destructive points of measurement will enable us not only to measure the beam sizes very quickly, but also to compare each of the four independent lasers that provide the beam to each experimental end-station. It will also be a means of quantitatively monitoring changes in the emittance consequent to machine drift or intentional changes to the front end setup.

## FIRST ASSEMBLY IN ARC 7

### *Optical-Mechanical Design*

The first of the four SLMs was designed and was installed during the last scheduled accelerator maintenance period. The SLM vacuum chamber was designed to replace a 1.1 m long 76.2 mm diameter drift pipe to simplify the installation. The vacuum chamber is supported by an extruded aluminum stand that straddles the ARC 9 beam tube below, which can be seen in Fig. 3. The assembly also has provisions for translation and rotation about three axes. The chamber consists of three sections separated by DIN125 conflat flanges. The first section has a 101.6 mm diameter bellows whose center is offset from the flange center-line. The second section is a 127 mm diameter tube with two welded support plates on the bottom and two optical rail mounting pads on the top. The third section contains two output tube ports, one on beamline center to pass the electrons and the other angled to extract the synchrotron light. Both DIN125CFs are pinned to limit the rotation in the event that the flanges have to be separated.

The initial optical layout has two achromatic lenses (focal lengths 400 mm and 100 mm), two turning mirrors, three filter wheels and a GigE Prosilica GC-650 [9] camera. The lenses will image a 20 mm wide object on the 659$x$493 pixel

ISBN: 978-3-95450-204-2 ISSN: 2673-5350 doi:10.18429/JACoW-IBIC2019-TUPP044

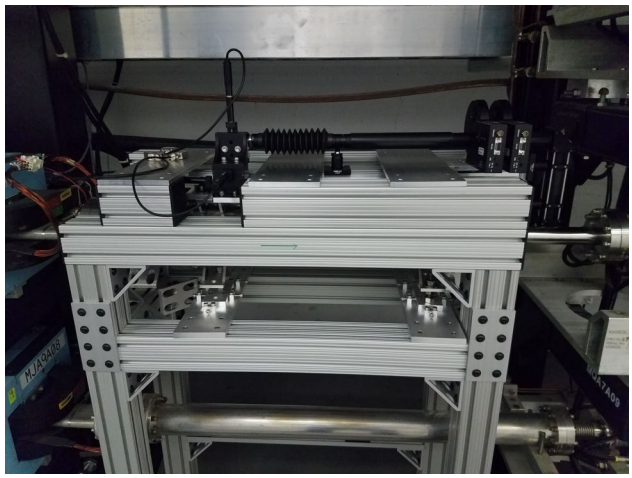

Figure 3: SLM installed in CEBAF tunnel. Aluminum support structure is used for minimal radiation shielding to protect the camera and other electronics.

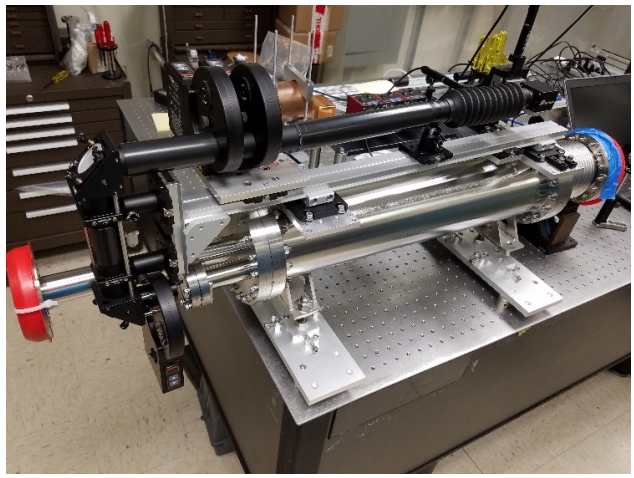

Figure 4: SLM in lab, for initial alignment of optical components.

camera sensor. The camera has a 7.4 µm square pixel and will illuminate 26 pixels for an 800 µm object. The 800 µm object size corresponds to a four sigma beam size. For the first installation, we installed three remote controlled six or twelve-position wheels for flexibility and experimentation. The remaining three assemblies will have fewer. The first wheel contains five slits ranging in widths from 0.75 mm to 6.00 mm and an open position. The second wheel has two open positions, a 410 nm bandpass filter, a 690 nm bandpass filter and two polarizers, one with a horizontal and the other a vertical orientation. The last wheel holds eleven neutral density filters from an OD of 0.1 to 4.0 as well as an open position. The camera is on an XYZ motorized translation stage with 12.7 mm motion in each axis to allow for remote alignment if necessary. All the optical components are mounted on a common rail with two rail carriers that register on the top pads of the vacuum chamber.

Initial alignment was performed on an optical table in the Diagnostics Lab. Team members from the Survey and Alignment (S&A) group used a FaroArm [10] to align a target and two size adjustable apertures. These apertures were used later to align a laser pointer to facilitate the alignment of the optical elements and focus of the camera sensor. The FaroArm was also used to align the vessel and to record the relative position of the fiducials on the chamber's top pads. A picture of the assembly in the Diagnostics Lab can be seen in Fig. 4. After alignment, the optics rail was removed and the vessel was installed in ARC 7. S&A had only to align the vessel relative to the dipole using the fiducials. The optic rail was then installed on the chamber just using the registers. First light on the SLM placed the image nearly in the center of the camera with no remote adjustment needed, corresponding to installation alignment at the level of 1 milliradian. Figure 5 shows the spot on the camera after initial beam through the Arc.

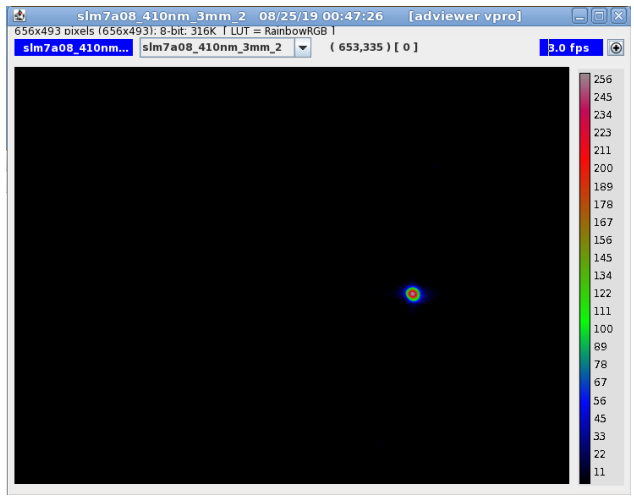


Figure 5: First installed SLM in Arc 7. Spot observed upon initial beam into the Arc after installation, no translation of camera was needed.

### *Single SLM Quad Scan Exercise*

After some initial calibration tests, a real time beam measurement was executed following the same protocol used with the wire scanners. One can see in Fig. 6 that the measured do not match the design values. Some of this could be due to the errors described below that have not yet been included. Figure 6 shows an example plot that is produced from such data. Software is currently under development that allows the user to automatically scan the quadrupole and fit each profile to a Gaussian function,

$$G(x) = a + b \cdot \exp\left(-(x-\mu)^2/2\sigma^2\right).$$

The software will also produce an SDDS [5] file that can be used in the `analyzer` [4], which is our current tool for analyzing quadrupole scans taken with wire scanners. The tool will also calculate the Twiss parameters, provide you calculated vs. design Twiss parameters, and allow one to

ISBN: 978-3-95450-204-2 ISSN: 2673-5350 doi:10.18429/JACoW-IBIC2019-TUPP044



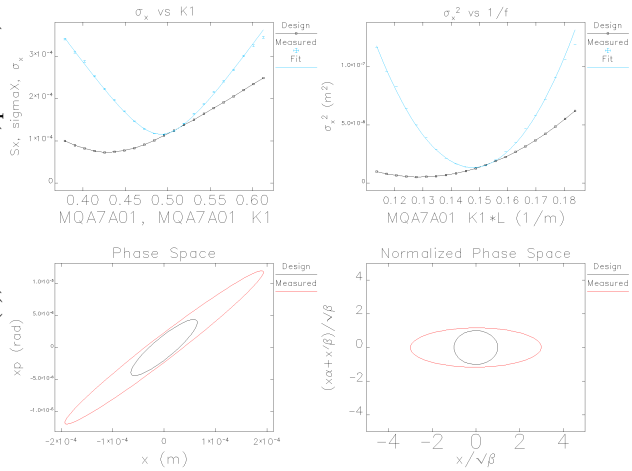


Figure 6: SLM quadrupole scan data plotted by the `analyzer` tool. Design values are also plotted for comparison.

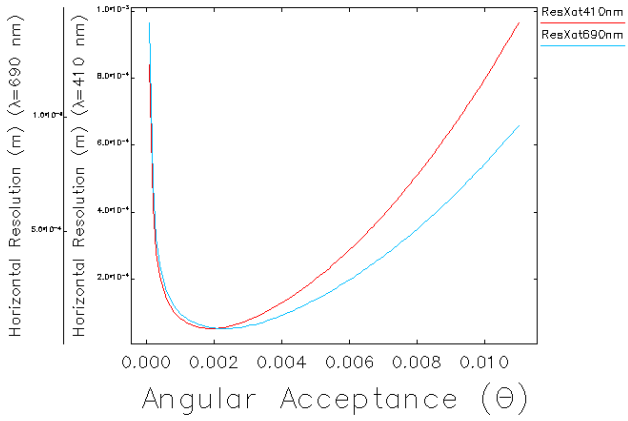


Figure 7: Horizontal Resolution as a function of Angular Acceptance.

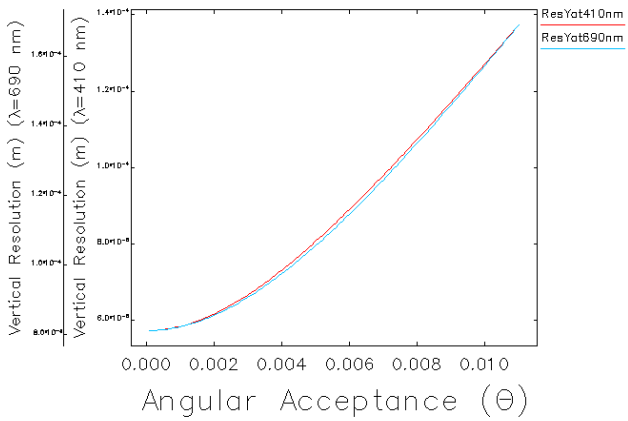


Figure 8: Vertical Resolution as a function of Angular Acceptance.

view each profile, to exclude selected points in the file, and to display phase space plots.

### *Resolution and Error Corrections*

Certain corrections to the spot size still need to be included in the software for analysis. Corrections discussed in Reference [11] include:

1. Chromatic Error, due to the light not being monochromatic. This error is reduced by using band-pass filters and achromatic lenses.

2. Depth of Field $\Delta_{df} \approx (L/2)\,\theta$, where $L$ is the length of the source and $\theta$ is the half-acceptance angle.

3. Diffraction Error from a vertical slit $\Delta_{diff} = 0.5\lambda/\theta$, where $\lambda$ is the wavelength of light that is imaged and $\theta$ is our half-angle of acceptance.

4. Curvature Error $\Delta_{curv} \approx R\theta^2/2$, where $R$ is the radius of bend $\theta$ is the same half-angle of acceptance. This correction is only needed in the plane of the bend, which in our case is in the horizontal plane.

5. Other errors include non-linear camera response (gamma-factor) and miscellaneous calibration errors.

For a given wavelength, one can optimize the half-acceptance angle to achieve the best resolution, minimizing the sum of the squares for the errors $\Delta_{df}$, $\Delta_{diff}$, and $\Delta_{curv}$ [11] described above.

Minimizing the errors, gives us an angular acceptance of about 1.5 mrad and a resolution of about 60 µm in x and y for the 410 nm vertical slit. Figures 7 and 8 show a comparison of the resolutions in x and y when comparing the 410 nm and the 690 nm band-pass filters.

## CONCLUSIONS

A method of measuring, matching, and monitoring four homologous points in the optical lattice of one of the ten CEBAF Arcs has been presented. The four point method should provide a quick, non-destructive method of measuring the beam profiles. Results from the first of the four have enabled testing of the optical design of the SLM assembly and the continuation of software development. There is much work left to do. The next steps include some simulation in `elegant`, as well as further analyzing the actual application of the methods for solving for the Twiss parameters.

## ACKNOWLEDGMENTS

This material is based upon work supported by the U.S. Department of Energy, Office of Science, Office of Nuclear Physics under contract DE-AC05-06OR23177.

ISBN: 978-3-95450-204-2 ISSN: 2673-5350 doi:10.18429/JACoW-IBIC2019-TUPP044

## REFERENCES


[1] P. Kloppel, "Transverse Emittance Measured by Synchrotron Light Monitor", CEBAF-TN-86-0026, 1986.

[2] M. M. Ali and M. G. Tiefenback, "Bunch Length Measurements using Synchrotron Light Monitor", in *Proc. IPAC'15*, Richmond, VA, USA, May 2015, pp. 1143–1145. doi:10.18429/JACoW-IPAC2015-MOPWI002

[3] M. G. Minty, F. Zimmermann, *Measurement and Control of Charged Particle Beams*, Berlin, Germany: Springer, 2012.

[4] D. L. Turner, "Software Tools for Emittance Measurement and Matching for 12 GeV CEBAF", in *Proc. IPAC'16*, Busan, Korea, May 2016, pp. 2792–2795. doi:10.18429/JACoW-IPAC2016-WEPOR053

[5] M. Borland, "A Self-Describing File Protocol for Simulation Integration and Shared Post-Processors", in *Proc. PAC'95*, Dallas, TX, USA, May 1995, paper WAE11, pp. 2184–2186.

[6] M. Borland, "elegant: A Flexible SDDS-Compliant Code for Accelerator Simulation", LS-287, in *Proc. ICAP'00*, Darmstadt, Germany, Sep. 2000, paper LS-287.

[7] A. Faus-Golfe *et al.*, "Multi-OTR System for ATF2," Physics Procedia, vol. 37, pp. 2072–2079, 2012. doi:10.1016/j.phpro.2012.02.525

[8] F. Lohl, "Measurements of the transverse emittance at the VUV-FEL", Diploma Thesis, Universität Hamburg, Hamburg, Germany, 2005. doi:10.3204/DESY-THESIS-2005-014

[9] Allied Vision Technologies, "Prosilica GC-650 product information", www.alliedvision.com/en/products/cameras/detail/Prosilica%20GC/650.html

[10] FARO, www.faro.com/products/3d-manufacturing/faroarm/applications/.

[11] J. A. Clarke, "A Review of Optical Diagnostics Techniques for Beam Profile Measurements", in *Proc. EPAC'94*, London, UK, Jun.-Jul. 1994, pp. 1643–1646.